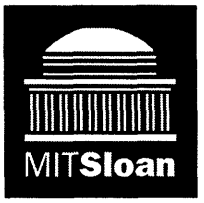

Massachusetts Institute of Technology

Sloan School of Management

Working Paper

Dynamic Optimization of a Linear-Quadratic Model with Incomplete Repair and Volume-Dependent Sensitivity and Repopulation

Lawrence M. Wein
Jonathan E. Cohen

June 1999
Working Paper Number 4071

Contact Address:
Prof. Lawrence M.Wein
Sloan School of Management
Massachusetts Institute of Technology
Cambridge, MA 02142-1343

Lwein@mit.edu

Dynamic Optimization of a Linear-Quadratic Model with Incomplete Repair and Volume-Dependent Sensitivity and Repopulation

Lawrence M. Wein, Ph.D.
Sloan School of Management, MIT, Cambridge, MA, USA

and

Jonathan E. Cohen, B.S.
Operations Research Center, MIT, Cambridge, MA, USA

Corresponding Author:

Lawrence M. Wein
Sloan School of Management, E53-343
MIT
Cambridge, MA 02142, USA
Phone: 617-253-6697
Fax: 617-258-7579
Email: lwein@mit.edu

Running title: Dynamic Optimization of a Linear-Quadratic Model

Abstract

Purpose: The linear-quadratic model typically assumes that tumor sensitivity and repopulation are constant over the time course of radiotherapy. However, evidence suggests that the growth fraction increases and the cell loss factor decreases as the tumor shrinks. We investigate whether this evolution in tumor geometry, as well as the irregular time intervals between fractions in conventional hyperfractionation schemes, can be exploited by fractionation schedules that employ time-varying fraction sizes.

Methods: We construct a mathematical model of a spherical tumor with a hypoxic core and a viable rim, and embed this model into the traditional linear-quadratic model by assuming instantaneous reoxygenation. Dynamic programming is used to numerically compute the fractionation regimen that maximizes the tumor control probability (TCP) subject to constraints on the biologically effective dose of the early and late tissues.

Results: In a numerical example that employs 10 fractions per week, optimally varying the fraction sizes increases the TCP from 0.7 to 0.966, and the optimal regimen incorporates large Friday afternoon doses that are escalated throughout the course of treatment, and larger afternoon doses than morning doses.

Conclusions: Numerical results suggest that a significant increase in tumor cure can be achieved by allowing the fraction sizes to vary throughout the course of treatment. Several strategies deserve further investigation: using larger fractions before overnight and weekend breaks, and escalating the dose (particularly on Friday afternoons) throughout the course of treatment.

Key Words: Dynamic optimization, Linear-quadratic, Reoxygenation, Repair, Repopulation.

Introduction

The linear-quadratic (LQ) model [1, 2] has gained relatively widespread acceptance among radiobiologists and clinicians as a tool for understanding radiation survival response. Current variants of the "LQ+time" model [3] capture two of the "four Rs" [4] of radiotherapy: repair (of sublethal damage) [5] and repopulation [1, 6]. A third R, redistribution (in the mitotic cycle), has been studied analytically [7, 8] and numerically [9]-[12]. However, it is unclear whether this factor can be exploited to obtain an improved therapeutic advantage [13]. The final R, reoxygenation, has only recently been directly modeled in the context of the LQ model [14], and has instead been incorporated via an exponential decay over time (independent of therapy) of the cell loss factor [15] or by modeling the resensitization process [8, 16, 17], which includes redistribution and reoxygenation.

The LQ model has been used to rationalize and refine hyperfractionation schemes that exploit the differential in α/β between early- and late-responding tissues [18, 19], and to assess accelerated protocols that attempt to mitigate the effects of repopulation [20]. More recently, the temporal – or dynamic – optimization of a LQ model with different repair rates for early and late tissues has generated a further therapeutic advantage by incorporating acute fractions at the beginning and end of treatment [21].

Our study was stimulated by two perceived gaps in the LQ literature. The first gap is that the elegant analysis in [21] appears to be the only study that systematically investigates the dynamic optimization of the LQ model. It focuses on accelerated regimens (e.g., brachytherapy), and the use of temporal optimization to exploit the irregular time intervals present in traditional non-accelerated protocols has yet to be studied. The second gap is the failure of the LQ model to capture the dynamics of reoxygenation and repopulation throughout the course of treatment. These two gaps are closely related, because *in vitro* and *in vivo* evidence suggests that the evolution of tumor geometry during radiation treatment and its

impact on radiosensitivity and repopulation can be exploited by time-varying fractionation regimens to further improve the therapeutic ratio. More specifically, hypoxic cells play a key role in the reduced response to radiation [22]-[24]. As a tumor shrinks during the course of therapy, diffusion-limited hypoxia decreases and necrotic regions become smaller and may eventually vanish. Moreover, as explained in [25] and demonstrated for spheroids in [26], nutrient-deprived cells are less apt to undergo mitosis, and the necrotic debris is eventually removed; consequently, the net repopulation rate increases as the tumor shrinks. Unfortunately, the LQ model – which typically assumes that the sensitivity and repopulation rate of a tumor are constant throughout the course of therapy – does not appear to be capable of tackling these issues, except within the context of a large simulation model [27]. In a related paper, O'Donoghue [28] ignores incomplete repair but develops a nonspatial model where the tumor grows exponentially when it is small and Gompertzian when it is big. He uses this model to investigate the tradeoff between duration of remission and tumor control probability.

The goal of this paper is two-fold: to incorporate the volume-dependent sensitivity and repopulation effects into a computationally-tractable, parsimonious LQ model, and to investigate whether radiotherapy protocols that employ time-varying dose rates can lead to an improved therapeutic ratio. To this end, a volume-dependent LQ model is constructed from an idealized spherical tumor model that contains a hypoxic core and a viable rim. Dynamic programming is used to solve the following optimal control problem: choose the radiotherapy protocol (a sequence of fractions of varying sizes) to maximize the tumor control probability, subject to a constraint on the biologically effective dose of the early and late tissues. A computational study is performed to assess the relative efficacy of dynamic fractionation schedules to exploit: (i) the irregular spacing of fractions (due to weekend breaks and intra-day vs. inter-day differences), (ii) the difference in repair rates between tumors

and tissues, and (iii) the evolution of the tumor geometry.

Methods

Model formulation

The model formulation is presented in four steps: (i) the description of the tumor geometry, (ii) the specification of a cell's sensitivity and repopulation as a function of its location within a tumor, (iii) the calculation of a tumor's overall sensitivity and rate of repopulation, and (iv) the construction of an equivalent ordinary differential equation (ODE) model.

Tumor geometry. We consider a spherical tumor that consists of a hypoxic core and a viable rim. The tumor's size is defined by its radius R, which changes over time as a result of radiation killing, necrotic loss and repopulation. If the current radius R is less than r_0, then the tumor contains no hypoxic core. If $R \geq r_0$ then the viable rim consists of the outer shell of thickness r_0 and the hypoxic core is the inner sphere of radius $R - r_0$. The cell density is assumed to be constant throughout the entire tumor. The spherical mathematical model can be thought of as a representation of a multicellular tumor spheroid [29] or as a grossly simplified caricature of a solid tumor *in vivo*. A similar approach – yielding qualitatively similar results – can be employed with other tumor geometries for other forms of cancer (e.g., a cord with a hypoxic center for squamous carcinoma [30]).

Location-dependent sensitivity and repopulation. In our model, a cell's sensitivity (α, β) and its net repopulation rate (γ) depends upon its radial distance, r, from the center of the tumor, and on the current tumor radius, R, where $r \in [0, R]$. All three quantities, which will be defined by $\alpha(r, R)$, $\beta(r, R)$ and $\gamma(r, R)$, take on a fixed well-oxygenated level (denoted by α_0, β_0 and γ_0) at the tumor surface (i.e., $r = R$) and decrease linearly as r decreases. If $R > r_0$ then all three parameters drop to zero at the outer edge of the hypoxic core (i.e., $r = R - r_0$). Furthermore, cells in the hypoxic core are insensitive to radiation,

do not repopulate, and are lost (i.e., necrotic debris is removed) at rate γ_N per unit time.

Hence, if $R < r_0$ then

$$\alpha(r,R) = \alpha_0 - \frac{\alpha_0}{r_0}(R-r), \quad \beta(r,R) = \beta_0 - \frac{\beta_0}{r_0}(R-r), \quad \gamma(r,R) = \gamma_0 - \frac{\gamma_0}{r_0}(R-r) \tag{1}$$

for $r \in [0,R]$. If $R > r_0$ then

$$\alpha(r,R) = 0, \quad \beta(r,R) = 0, \quad \gamma(r,R) = -\gamma_N \tag{2}$$

for $r \in [0, R-r_0]$, and

$$\alpha(r,R) = \frac{\alpha_0}{r_0}(r-R+r_0), \quad \beta(r,R) = \frac{\beta_0}{r_0}(r-R+r_0), \quad \gamma(r,R) = \frac{\gamma_0}{r_0}(r-R+r_0) \tag{3}$$

for $r \in (R-r_0, R]$.

A simpler variant (where the growth fraction is constant throughout the viable rim) of this "constant crust" model has been shown to capture the *in vitro* growth characteristics of multicellular tumor spheroids for several tumor lines [31]. Moreover, experimental evidence shows that the growth fraction [32] and sensitivity [30] in solid tumors decrease as the distance from the nutrient supply increases. Nonetheless, the constant crust model and the linear functions in (1)-(3) were chosen for their parsimony (only five parameters are required) and computational tractability, and the *in vitro* and *in vivo* situation is considerably more complex. The composite function [14, 33] resulting from radiosensitivity as an empirically-derived function of oxygen level [34] and oxygen level as a function of radial location (via radial inward diffusion in a cylinder [30]) has a sigmoid shape in the viable rim. Similarly, while experiments [35] suggest that repopulation may be roughly linear in the oxygen level, the resulting composite function of repopulation in terms of radius is nonlinear. Incorporating these composite functions would add a considerable number of parameters and cause the subsequent analysis to be extremely tedious, while generating little or no change in our qualitative results.

A tumor's overall sensitivity and repopulation rate. The spherical tumor model presented thus far consists of a heterogeneous collection of cells of varying radiation sensitivity and mitosis capability. We model radiation killing using the LQ+time formula [1]. If $f(\alpha,\beta,\gamma)$ is the joint probability density function of the three parameters for the various cells in a tumor of fixed size (the dependence on tumor radius R is suppressed in equations (4)-(5) below), then the expected surviving fraction of cells after a dose of size d given over the infinitesimal interval of time Δt is $\int e^{-\alpha d-\beta d^2+\gamma\Delta t} f(\alpha,\beta,\gamma)d\alpha d\beta d\gamma$ [36]. Rather than calculate this expectation exactly, we follow the approach in [17] and employ two Taylor series approximations. The approximation $e^x \approx 1+x+\frac{x^2}{2}$ yields

$$\ln E[\exp(-\alpha d-\beta d^2+\gamma\Delta t)] \approx \ln E\left[1-\alpha d-\beta d^2+\gamma\Delta t+\frac{[\gamma\Delta t-\alpha d-\beta d^2]^2}{2}\right]. \quad (4)$$

Using the approximation $\ln x \approx (x-1)-\frac{(x-1)^2}{2}$ in equation (4) and ignoring all polynomial terms of order 3 and higher (i.e., d^3, $d^2\Delta t$, $d(\Delta t)^2$, $(\Delta t)^3$) and the $(\Delta t)^2$ term, we get

$$\ln E[\exp(-\alpha d-\beta d^2+\gamma\Delta t)] \approx -\bar{\alpha}d-\bar{\beta}d^2+\bar{\gamma}\Delta t+\frac{\sigma_\alpha^2 d^2}{2}, \quad (5)$$

where $\bar{\alpha}$, $\bar{\beta}$ and $\bar{\gamma}$ denote the means and σ_α^2 is the variance of α. Numerical results not reported here show that the approximation in (5) is very accurate. By equation (5),, the effective values of α, β and γ are given by $\bar{\alpha}$, $\bar{\beta}-\frac{\sigma_\alpha^2}{2}$ and $\bar{\gamma}$, respectively. These quantities will be referred to as $\alpha(R)$, $\beta(R)$ and $\gamma(R)$, and can be derived by integrating the functions in (1)-(3) over $\frac{3r^2}{R^3}$ (i.e., the surface area at radius r divided by the total volume) from $r=0$ to $r=R$:

$$\alpha(R) = \alpha_0\left(1-\frac{R}{4r_0}+\frac{[(R-r_0)^+]^4}{4r_0R^3}\right), \quad (6)$$

$$\beta(R) = \beta_0\left(1-\frac{R}{4r_0}+\frac{[(R-r_0)^+]^4}{4r_0R^3}\right)-\frac{3\alpha_0^2R^2}{160r_0^2}$$
$$+\frac{\alpha_0^2(R-r_0)^2}{2r_0^2}\left(\frac{3}{8}\left[\left(1-\frac{r_0}{R}\right)^+\right]^2-\frac{2}{5}\left[\left(1-\frac{r_0}{R}\right)^+\right]^3+\frac{1}{16}\left[\left(1-\frac{r_0}{R}\right)^+\right]^6\right), \quad (7)$$

$$\gamma(R) = \gamma_0\left[1-\frac{R}{4r_0}+\frac{[(R-r_0)^+]^4}{4r_0R^3}\right]-\gamma_N\left[\left(1-\frac{r_0}{R}\right)^+\right]^3. \quad (8)$$

The equivalent ODE. Suppose an arbitrary dose rate d_t is applied over the time interval $[0, T]$. The surviving fraction of cells under the traditional (i.e., constant α and β and $\gamma = 0$) LQ model with incomplete repair (with repair rate μ) is

$$\exp\Big(-\alpha \int_0^T d_t dt - 2\beta \int_0^T d_t \Big(\int_0^t d_s e^{-\mu(t-s)} ds\Big) dt\Big). \tag{9}$$

Expression (9) can be derived by various means (see equation (8) in [37] and references therein) when α and β are constant. To obtain an analogous result for volume-dependent sensitivity (α_t, β_t) and repopulation (γ_t), we use the ODE model [2, 37]

$$\dot{n}_t = [\gamma_t - \alpha_t d_t - \frac{1}{2} k u_t^2] n_t, \tag{10}$$

$$\dot{u}_t = c_t d_t - \mu u_t - 2k u_t^2, \tag{11}$$

where n_t is the number of cells at time t, u_t is the number of DNA double-strand breaks per cell that are susceptible to enzymatic processing. The breaks can come together in pairwise interactions at rate ku_t^2, with half of these interactions clonogetically fatal. Double strand breaks are induced at a rate of c_t per unit dose at time t and repaired at rate μ. A minor generalization of existing results (for the case $\alpha_t = \alpha$, $\beta_t = \beta$, $\gamma_t = 0$) gives a surviving fraction (after all enzymatic processing is complete) equal to

$$\frac{n_T}{n_0} = \exp\Big(-\int_0^T \alpha_t d_t dt - \frac{k}{2\mu} \int_0^T c_t d_t \big(\imath n t_0^t c_s d_s e^{-\mu(t-s)} ds\big) dt + \int_0^T \gamma_t dt\Big). \tag{12}$$

For the case ($\alpha_t = \alpha$, $c_t = c$, $\gamma_t = 0$), equation (12) reduces to equation (9) and $\beta = \frac{c^2 k}{4\mu}$. To capture volume-dependent sensitivity and repopulation, we let R_t be the tumor radius at time t and substitute (from equations (6)-(8), respectively) $\alpha(R_t)$ for α_t, $\sqrt{\frac{4\mu\beta(R_t)}{k}}$ for c_t, and $\gamma(R_t)$ for γ_t in equation (12). With these substitutions, equation (12) can be expressed as the differential equation

$$\dot{n}_t = n_t[\gamma(R_t) - \alpha(R_t) d_t - 2\sqrt{\beta(R_t)} d_t \int_0^t \sqrt{\beta(R_s)} d_s e^{-\mu(t-s)} ds]. \tag{13}$$

Equation (13) assumes that as the tumor dynamically shrinks (from radiation and hypoxic loss) and grows (from repopulation), the cells instantaneously reconfigure themselves and change their sensitivity and repopulation parameters. Empirical evidence [38] suggests that the quickness of chronic reoxygenation varies considerably for different experimental animal tumors, although this process is generally considered to occur faster than tumor shrinkage and growth. This "instantaneous reoxygenation" assumption is not too objectionable because the computational study only considers protocols that have at least eight hours between fractions.

Because the sensitivity and repopulation functions are expressed in terms of the radius, we need to express the differential equation in terms of the radius, not the number of cells. If we let θ be the density of cells per unit volume in the spherical tumor, then $n_t = \frac{4}{3}\theta\pi R_t^3$ and $\dot{n}_t = \frac{dn_t}{dR_t}\dot{R}_t = 4\theta\pi R_t^2\dot{R}_t$. Substituting these expressions and (6)-(8) into (13) yields the differential equation

$$\dot{R}_t = \frac{R_t}{3}[\gamma(R_t) - \alpha(R_t)d_t - 2\sqrt{\beta(R_t)}d_t\int_0^t \sqrt{\beta(R_s)}d_s e^{-\mu(t-s)}ds]. \tag{14}$$

This equation forms the basis of the optimal control problem.

Problem formulation

The optimization problem is to choose a radiation schedule that maximizes the tumor control probability (TCP), subject to a constraint on the biologically effective dose (BED) [39] of the early and late tissues. We employ the commonly used "Poisson model" [40], which states that the TCP is e^{-C_T}, where C_T is the number of clonogens (i.e., cells capable of tumor regeneration) at the end of treatment. We assume that clonogens make up a fixed proportion, p, of the tumor cells and that clonogens' sensitivity to radiation is no different than other tumor cells. Mathematically, the problem is to choose T and $\{d_t \geq 0, 0 \leq t \leq T\}$ to maximize

$$\exp\left(-\frac{4\theta\pi p}{3}(R_T^3 - [(R_T - r_0)^+]^3)\right) \tag{15}$$

subject to (14),

$$\int_0^T d_t dt + \frac{2}{k_L}\int_0^T d_t \int_0^t d_s e^{-\mu_L(t-s)} ds dt \leq D_L, \tag{16}$$

and

$$D_t - \inf_{0\leq s\leq t} D_s \leq D_E \quad \text{for} \quad 0 \leq t \leq T, \tag{17}$$

where

$$D_t = \int_0^t d_s ds + \frac{2}{k_E}\int_0^t d_s \int_0^s d_u e^{-\mu_E(s-u)} du ds - \frac{\gamma_E}{\alpha_E} t, \tag{18}$$

k_E, μ_E, γ_E and D_E are the α/β ratio, repair rate, repopulation rate and BED, respectively, for the early tissue, and k_L, μ_L and D_L are the corresponding quantities for the late tissue. We assume that these parameters are constant and that the late tissue does not repopulate. Note that the late tissue constraint (16) only needs to be assessed at time T, whereas the early tissue constraint (17) needs to be imposed throughout the course of treatment. The reflection mapping on the left side of (17) (referred to as the "one-sided regulator" in [41]; here, "inf" is the infimum, or minimum) is needed to prevent the early tissue from "storing" negative BED in between fractions. Also, when we refer to the early constraint as "binding", we mean that it is satisfied with equality on Friday afternoons.

Solution to the control problem

Pontryagin's maximum principle [42] is the most widely used method for solving deterministic optimal control problems. By expressing each of equations (14), (16) and (18) as two ordinary differential equations (e.g., for (14), let $Y_t = \int_0^t \sqrt{\beta(R_s)} d_s e^{-\mu(t-s)} ds$ so that $\dot{Y}_t = \sqrt{\beta(R_t)} d_t - \mu Y_t$), it can be shown that the Hamiltonian H is linear in the control d_t. Therefore, the control problem is singular and we have shown that the singularity is of order one (§6-21 of [43]). In the case where there is no early tissue constraint, we have solved the equations $H = 0$ (because the treatment duration T is a decision variable) and $\frac{d^2}{dt^2}\left(\frac{\partial H}{\partial d_t}\right) = 0$ to find d_t in terms of the various state and adjoint variables, but the resulting expressions are too complex to derive any fundamental insights into the nature of the opti-

mal solution; hence, this analysis is omitted. The early tissue constraint makes this control problem extremely complex because it needs to be evaluated at each point in time (or after each fraction if a fractionation scheme is employed). Hence, in the Results section, we resort to solving problem (14)-(18) numerically using an iterative dynamic programming algorithm constructed exclusively for singular control problems [44].

Results

Optimal static scheme

We restrict our numerical study to fractionation schemes that have 10 fractions per week. More specifically, time $t = 0$ corresponds to the first fraction given on Monday morning, there are two fractions per day that are separated by eight hours (each fraction's duration is one minute), and there is no treatment on the weekends. To assess the efficacy of the optimal solution to (14)-(18), we compare it to the best static (i.e., fraction sizes do not vary over time) scheme, which is characterized by the fraction size and the total number of fractions. The optimal design of static regimens can be viewed graphically as the problem of maximizing a nonlinear objective (TCP) subject to satisfying two inequality (BED) constraints, as shown in Figure 1. We assume that the hyperfractionation (HF) regimen (70 fractions $\times$ 1.15 Gy) is the optimal (i.e., it solves problem (14)-(18)) scheme among static policies with 10 fractions per week. We also assume that the late and early BED constraints (16)-(17) are binding under HF and the resulting TCP in (15) is 0.7.

Parameter values

The 15 parameters and one initial condition in the optimization problem are found by the following procedure. First, the initial tumor radius R_0 is set equal to 0.5 cm, which corresponds to a typical tumor at the time of presentation. We set the viable rim radius r_0 equal to 0.05 cm, which is about three times larger than the oxygen diffusion limit in tumor tissue [30], in order to reflect the fact that a tumor of this size would be vascularized [45].

This value leads to 27.1% of the tumor being viable initially. The cell density $\theta = \frac{3q}{4\pi R_c^3}$, where q is the packing factor and R_c is the cell radius. If $q = 0.4$ and $R_c = 10\mu$m [46], then the density is $\frac{3}{\pi} \times 10^8$ cells/cm^3, and we use $\theta = 10^8$ cells/cm^3. The loss rate for necrotic debris is taken to be $\gamma_N = \frac{1}{48}$ hr^{-1} [47]. The tumor repopulation parameter is chosen so that the steady-state tumor radius without radiation is $2R_0 = 1.0$ cm, giving $\gamma_0 = 0.256$ hr^{-1}. Five parameter values are taken from Brenner et al. [21]: $k_E = 10$ Gy, $k_L = 4$ Gy, $\mu = \mu_E = \frac{\ln 2}{0.5}$ hr^{-1} and $\mu_L = \frac{\ln 2}{4}$ hr^{-1}. By Table II of [48] (but using a D_{prolif} of 1.6 Gy/day rather than 1.8 Gy/day), we set $\frac{\gamma_E}{\alpha_E} = 1.6$ Gy/day$[1 + (2$ Gy$)k_E] = 0.08$ Gy/hr.

This leaves five unassigned parameters, α_0, β_0, D_L, D_E and p, which are determined using our assumptions about HF described earlier. We set $D_L = 111.5$ Gy and $D_E = 4.59$ Gy, which are the resulting BED values under HF. The parameter $\beta_0 = 1.78$ Gy^{-2} is set so that the time average ratio of $\frac{\alpha(R)}{\beta(R)}$ over the course of HF is 10. The parameter $\alpha_0 = 2.5$ Gy^{-1} is set so that HF is the optimal static fractionation scheme (as determined by an exhaustive search over the number of doses and dose size, with a dose discretization of 0.05 Gy), and $p = 2.15 \times 10^{-7}$ (which is smaller than most estimates in the literature) is set so that HF achieves a TCP of 0.7.

Numerical Results

The optimal solution to (14)-(18) (using a dose discretization of 0.05 Gy) is displayed in Figure 2. This scheme administers a total of 66.81 Gy in six weeks, and achieves a TCP of 0.966, which is a significant improvement over HF's TCP of 0.7. The resulting BED administered to the early and late tissues is 4.59 Gy and 98.5 Gy, respectively. Hence, the early constraint is binding under the optimal scheme but the late constraint has a slack of 13 Gy.

The optimal solution in Figure 2 possesses several interesting features. The most pronounced effect is the large doses on Friday afternoons. These six doses are over 3.5

times larger on average than the other 54 doses. These large fractions are primarily used to compensate for the weekend breaks. However, a secondary factor could be that tumors are also smaller on Friday afternoon than at other times of the week, and smaller tumors are more sensitive and may attract larger fractions. There is also a significant am-pm effect: 60.0% of the total dose on Monday through Thursdays is administered in the afternoons (including Friday in this calculation would introduce the weekend bias). These large afternoon fractions offset the repopulation during the 16-hour gap until the next morning's fraction. A third feature of Figure 2 is the intensification of the Friday afternoon doses throughout the course of treatment. The Friday afternoon fractions in the last three weeks of treatment are 16.8% larger on average than those in the first three weeks. This escalation over the course of treatment is due to the fact that $\alpha(R)$ increases and (to a lesser extent) $\frac{\alpha(R)}{\beta(R)}$ decreases as the tumor becomes smaller, making it more desirable to use larger fractions towards the end of treatment. (If $\frac{\alpha(R)}{\beta(R)}$ increased as the tumor shrank, there would be a tradeoff: larger doses towards the end of treatment would kill more tumor cells but also cause more late tissue damage.) Because of the early tissue constraint, the total dose given in each of the last three weeks is less than the total dose given in each of the first three weeks, in order to compensate for the larger Friday afternoon doses during the latter half of treatment. Finally, it is also worth noting that the optimal policy ends on a Friday. Because the value of D_E is so low, the early tissue tends to nearly heal itself over each weekend, and by ending on a Friday the optimal scheme makes sure to exhaust the allowable early BED.

The large first dose observed by Brenner et al. [21] is absent from Figure 2. This is probably because the early constraint forces the optimization procedure to choose between a large Monday morning fraction or a large Friday afternoon fraction in the first week, and apparently the Friday dose is more efficacious. The absence of the large first dose may also be due to the fact that we are focusing on traditional (i.e., 10 fractions per week)

hyperfractionation schemes, whereas Brenner et al. [21] considered accelerated protocols.

Discussion

The foundation of the rationale for current fractionation schemes is the exploitation of the differences in radiation sensitivity (α, β) and repopulation (γ) between the tumor and the normal (primarily late) tissue. More recent results [21] show how the difference in repair rates can also be exploited by temporally optimizing the dose rate in accelerated protocols. The results in the present paper complement these ideas by suggesting that the therapeutic ratio can be further improved by exploiting two other factors: irregular time intervals between doses caused by overnight and weekend breaks, and the changing radiosensitivity and repopulation rate of the tumor caused by reoxygenation. The weekend break was the most pronounced effect in our numerical example, causing Friday afternoon doses to be about 3.5 times larger than the other doses. The overnight effect was also significant, with afternoon doses accounting for 60.0% of the total dose administered on Mondays through Thursdays. The tumor increased its radiosensitivity and repopulation rates throughout the course of treatment, leading to 16.8% larger Friday afternoon doses in the latter three weeks of treatment than in the first three weeks of treatment. Sensitivity analysis (not reported here) shows that these three effects become stronger as the early tissue constraint is relaxed (i.e., D_E or $\frac{\gamma_E}{\alpha_E}$ is increased).

Figure 2 shows that the optimal fractionation scheme compensates for irregular time intervals between doses by administering larger doses before longer breaks and shorter doses before shorter breaks. We know of no previous work that systematically investigates this intuitively appealing strategy. Although our numerical study was restricted to hyperfraction schemes (10 fractions per week), this strategy may also improve conventional (five fractions per week) and accelerated (15 or 21 fractions per week) protocols.

The optimal radiation policy exploits the reoxygenation process by taking into account

the fact that as the tumor gets smaller in our volume-dependent LQ model, the tumor's sensitivity (α) increases and its $\frac{\alpha}{\beta}$ ratio decreases. Hence, giving large doses at the beginning of therapy is wasteful, since some of this dose can kill more cells if it is deferred until the tumor is smaller. Moreover, as the tumor shrinks, the growth fraction increases and the cell loss factor decreases, and consequently the repopulation rate increases. This provides an additional incentive to increase the dose rate (thereby reducing the length of treatment) when the tumor is smaller. In summary, an optimal radiation policy attempts to exercise patience when faced with a large tumor: it slowly and methodically chips away at the outer surface of the tumor, until the hypoxic core or the remaining available BED is sufficiently small, at which time the dose rate is increased until the end of treatment.

The dose intensification strategy suggested by our analysis has appeared in various guises in the mathematical radiobiology, clinical oncology and clinical radiotherapy literatures. In two mathematical papers [49, 50] that employ the single-hit multitarget model for oxygenated and anoxic cells, the numerically computed optimal solution has a dose size that increases over time, because the oxygenated fraction increases as the tumor gets smaller. These models do not attempt to capture the tumor geometry and – because these papers pre-date the widespread adoption of the LQ model – their handling of normal tissue is necessarily imprecise.

The Norton-Simon hypothesis [51, 52] has had a considerable impact on the thinking of the clinical oncology community. They use the log-kill assumption [53] (chemotherapy kills a fixed percentage of cells, not a fixed number of cells) and the Gompertzian growth assumption [54] (the repopulation rate decreases as the tumor gets larger) to argue for *intensification therapy*, where the chemotherapy dose level is increased as the tumor becomes smaller. Our reasoning is consistent with theirs, in that the mathematical tumor models such as the one posed here lead to Gompertzian growth over much of the tumor's life [31, 55].

Dose intensification throughout the course of treatment can also be seen in concomitant boost (CB) therapy, where daily 1.8 Gy fractions are given for six weeks to the standard large field, plus an additional 1.5 Gy fraction is delivered to a reduced field on a daily basis for the last 10-12 days of treatment. The boost appears to be more efficacious when administered late in treatment rather than early [56], which is consistent with our results. This regimen is currently being tested against conventional fractionation, hyperfractionation and split-course accelerated fractionation in the RTOG Trial 90-03. The rationale put forward for CB [57]-[59] is the reduction in overall time and the lower toxicity generated by the reduced field; however, Peters [59] mentions that the increased oxygenation and cell proliferation at the end of treatment may also aid in CB's superior performance.

Several studies [60]-[62] have proposed regimens in which daily doses are escalated throughout the course of treatment. However, the rationales provided for this approach are different than ours: these researchers wanted to overcome accelerated repopulation or stimulate early tissue repopulation during the early weeks of therapy so as to better tolerate the late treatment. The amount of escalation in [62] (from 1.2 Gy to 1.6 Gy) is of the same order of magnitude as the escalation of Friday afternoon doses in Figure 2.

The dose intensification strategy generated by our analysis also suggests how one would optimally schedule combination therapy of a hypoxic cytotoxin such as terapazamine [63] and radiation: the radiation dose would be increased and the terapazamine dose would be decreased throughout the course of therapy.

While most studies focus on the tradeoff of tumor and late tissues, we explicitly incorporate an early tissue constraint. Although this constraint is more difficult to express mathematically (see (17)-(18)) and more difficult to handle computationally than the late tissue constraint, its inclusion provides a more complete view of the problem. Indeed, the early tissue constraint was omitted in the initial phase of our research, and the resulting

optimal fractionation schedules would have been fatal to humans. Moreover, the early constraint allows one to graphically view the static fractionation protocol design problem as the constrained optimization problem in Figure 1. This graphical tool, which consists of plotting TCP iso-curves and BED constraints for early and late tissues, may help address important questions, such as which BED constraints (i.e., just one of them or both – note that the optimal solution need not be at the intersection of the two constraints) are binding in the optimal protocol for various types of tumors.

We conclude with several caveats. Our underlying tumor model is a reasonable one for prevascular tumors. It is well known [45] that tumors undergo the process of angiogenesis when they reach about 0.3 cm in diameter, at which time blood vessels are recruited from the surrounding tissue and a growth surge occurs. However, results of [64]-[66] show that the necrotic fraction and hypoxic fraction increase with the volume of vascularized tumors, and blood vessels are densest at the tumor periphery and are absent in the necrotic core. Hence, our simple model appears to capture the qualitative features of vascular tumors. Nevertheless, there have been studies suggesting that oxygenation may decrease during the course of fractionated radiation treatment [67]. Further research is needed to understand how α, $\frac{\alpha}{\beta}$ and γ vary *in vivo* over the course of radiotherapy.

We have attempted to add a degree of biological realism to the LQ model without imposing too many extra parameters. The LQ+time+incomplete repair model has four parameters and equations (6)-(8) and (14) have six parameters, the two additional ones being the thickness of the viable rim and the loss rate of necrotic debris. Hence, while our model is considerably more complex than the traditional LQ model, our use of one-parameter linear functions for sensitivity and repopulation leads to a relatively parsimonious, albeit simplistic, model. Nonetheless, our optimization problem (14)-(18) contains 15 parameters and consequently is nearly impossible to validate. Moreover, small changes in some parameters

(e.g., $\frac{\alpha_E}{\gamma_E}$ or D_E) lead to quite different quantitative (although similar qualitative) results. We also suspect that the actual TCP iso-curves are less flat than pictured in Figure 1 (exploratory calculations show that they are less flat in the traditional model, where α and β are constant; e.g., the 0.7 TCP iso-curve that passes through HF also passes through the 50×1.3 Gy protocol), which would lead to a smaller increase in TCP than the impressive numbers achieved by the regimen in Figure 2. For all these reasons, we put little stock in the precise quantitative results provided here, and the policy appearing in Figure 2 is not intended to be interpreted as the optimal dynamic HF schedule. Nevertheless, our results do suggest that there is untapped potential for the use of dynamic fractionation schemes that incorporate the overnight effect, the weekend effect and the dose escalation effect. Our hope is that these types of models and analyses will provide a systematic way of generating and refining approaches to improve the therapeutic ratio of radiotherapy by temporal optimization of dose schedules.

Acknowledgments

We thank Dr. Jeff Goldstein for helpful discussions and Amy Cohn for performing computational results during the early part of this research.

References

[1] Fowler JF. The linear-quadratic formula and progress in fractionated radiotherapy. *Br J Radiol* 1989;62:679-694.

[2] Thames HD, Hendry JH. Fractionation in radiotherapy. London: Taylor & Francis; 1987.

[3] Orton CG, Brenner DJ, Dale RG, *et al.* Radiobiology. In: Nag S, editor. High dose rate brachytherapy: A textbook. Armonk, NY: Futura; 1994. Chapter 2.

[4] Withers HR. Biological basis of radiation therapy for cancer. *Lancet* 1992;339:156-159.

[5] Thames HD. An 'incomplete repair' model for survival after fractionated and continuous irradiations. *Int J Radiat Biol* 1985;47:319-339.

[6] Travis EL, Tucker SL. Iso-effect models and fractionated radiation therapy. *Int J Radiat Oncol Biol Phys* 1987;13:283-287.

[7] Chen P-L, Brenner DJ, Sachs, RK. Ionizing radiation damage to cells: effects of cell cycle redistribution. *Math Biosc* 1995;126:147-170.

[8] Hahnfeldt P, Hlatky L. Resensitization due to redistribution of cells in the phases of the cell cycle during arbitrary radiation protocols. *Radiat Res* 1996;145:134-143.

[9] King CR, Nath R, Rockwell S. Effects of continuous low dose-rate irradiation: computer simulations. *Cell Tissue Kinet* 1988;21:339-351.

[10] Yakovlev AY, Zorin AV. Computer simulation in cell radiobiology. In: Lecture notes in biomathematics, Vol. 74. Berlin and New York: Springer-Verlag; 1988.

[11] Dillehay LE. A model of cell killing by low-dose-rate radiation including repair of sublethal damage, G_2 block, and cell division. *Radiat Res* 1990;124:201-207.

[12] Zaider M, Wuu CS, Minerbo GN. The combined effects of sublethal damage repair, cellular repopulation and redistribution in the mitotic cycle. I. Survival probabilities after exposure to radiation. *Radiat Res* 1996;145:457-466.

[13] Steel GG. Cell synchronization unfortunately may not benefit cancer therapy. *Radioth Oncol* 1994;32:96-97.

[14] Wouters BG, Brown JM. Cells at intermediate oxygen levels can be more important than the "hypoxic fraction" in determining tumor response to fractionated radiotherapy. *Radiat Res* 1997;147:541-550.

[15] Jones B, Dale RG. Cell loss factors and the linear-quadratic model. *Radioth Oncol* 1995;37:136-139.

[16] Hlatky LR, Hahnfeldt P, Sachs RK. Influence of time-dependent, stochastic heterogeneity on the radiation response of a cell population. *Math Biosci* 1994;122:201-220.

[17] Brenner DJ, Hlatky LR, Hahnfeldt PJ, *et al.* A convenient extension of the linear-quadratic model to include redistribution and reoxygenation. *Int J Radiat Oncol Biol Phys* 1995;32:379-390.

[18] Withers HR, Peters LJ. Biologic aspects of radiation therapy. In: Gilbert GH, editor. Textbook of radiotherapy. Philadelphia: Lea and Feibiger; 1980. p.103-180.

[19] Withers HR, Peters LJ, Thames HD, *et al.* Hyperfractionation. *Int J Radiat Oncol Biol Phys* 1982;8:1807-1809.

[20] Fowler JF. How worthwhile are short schedules?: A series of exploratory calculations. *Radiother Oncol* 1990;18:165-181.

[21] Brenner DJ, Hall EJ, Huang Y, *et al.* Optimizing the time course of brachytherapy and other accelerated radiotherapeutic proptocols. *Int J Radiat Oncol Biol Phys* 1994;29:893-901.

[22] Gray LH, Conger AD, Ebert M, *et al.* The concentration of oxygen dissolved in tissues at the time of irradiation as a factor in radiotherapy. *Br J Radiol* 1953;26:638-648.

[23] Powers WE, Tolmach LJ. A multicomponent x-ray survival curve for mouse lymphosarcoma cells irradiated in vivo. *Nature* 1963;197:710-711.

[24] Thomlinson RH, Craddock EA. The gross response of an experimental tumour to single doses of X-rays. *Br J Cancer* 1967;21:108-123.

[25] Fowler JF. The phantom of tumor treatment - continually rapid proliferation unmasked. *Radioth Oncol* 1991;22:156-158.

[26] Sham E, Durand RE. Cell kinetics and repopulation during multifraction irradiation of spheroids. *Radiother Oncol* 1998;46:201-207.

[27] Duchting W, Ulmer W, Ginsberg T. Cancer: A challenge for control theory and computer modeling. *Europ J Cancer* 1996;32A:1283-1292.

[28] O'Donoghue JA. The response of tumours with Gompertzian growth characteristics to fractionated radiotherapy. *Int J Radiat Biol* 1997;72:325-339.

[29] Sutherland RM, McCredie JA, Inch WR. Growth of multicell spheroids in tissue culture as a model of nodular carcinoma. *J Natl Cancer Inst* 1971;46:113-120.

[30] Thomlinson RH, Gray LH. The histological structure of some human lung cancers and the possible implications for radiotherapy. *Br J Cancer* 1955;9:539-549.

[31] Conger AD, Ziskin MC. Growth of mammalian multicellular tumor spheroids. *Cancer Res* 1983;43:556-560.

[32] Tannock IF. The relation between cell proliferation and the vascular system in a transplanted mouse mammary tumor. *Br J Cancer* 1968;22:258-273.

[33] Tannock IF. Oxygen diffusion and the distribution of cellular radiosensitivity in tumors. *Br J Radiol* 1972;45:515-524.

[34] Alper T, Howard-Flanders P. The role of oxygen in modifying the radiosensitivity of *E. cole* B. *Nature* 1956;178:978-979.

[35] Froese G. The respiration of ascites tumor cells at low oxygen concentrations. *Biochem Biophys Acta* 1962;57:509-519.

[36] Schultheiss TE, Zagars GK, Peters LJ. An explanatory hypothesis for early- and late-effect parameter values in the LQ model. *Radioth Oncol* 1987;9:241-248.

[37] Sachs RK, Hahnfeld P, Brenner DJ. The link between low-LET dose-response relations and the underlying kinetics of damage production/repair/misrepair. *Int J Radiat Biol* 1997;72:351-374.

[38] Hall EJ. Radiobiology for the radiologist, 4th ed. Philadelphia: Lippincott; 1994.

[39] Barendsen GW. Dose fractionation, dose rate and iso-effect relationships for normal tissue responses. *Int J Radiat Oncol Biol Phys* 1982;8:1981-1997.

[40] Tucker SL, Taylor JMG. Improved models of tumour cure. *Int J Radiat Biol* 1996;70:539-553.

[41] Harrison JM. Brownian motion and stochastic flow systems. New York, NY: John Wiley and Sons; 1985.

[42] Pontryagin LS, Boltyanskii VG, Gamkrelidze RV, *et al.* The mathematical theory of optimal processes. New York: Interscience; 1962.

[43] Athans M, Falb PL. Optimal Control. New York: McGraw-Hill; 1966.

[44] Luus R. On the application of iterative dynamic programming to singular optimal control problems. *IEEE Trans Automatic Control* 1992;37:1802-1806.

[45] Folkman J. The vascularization of tumors. *Sci Am* 1976;234:58-73.

[46] O'Donoghue JA, Bardies M, Wheldon TE. Relationships between tumor size and curability for uniformly targeted therapy with beta-emitting radionuclides. *J Nuclear Med* 1995;36:1902-1909.

[47] Fowler JF. Potential for increasing the differential response between tumors and normal tissues: can proliferation rate be used? *Int J Radiat Oncol Biol Phys* 1986;12:641-645.

[48] Thames HD, Bentzen SM, Turesson I, *et al.* Time-dose factors in radiotherapy: a review of human data. *Radioth Oncol* 1990;19:219-235.

[49] Hethcote H, Waltman P. Theoretical determination of optimal treatment schedules for radiation therapy. *Radiat Res* 1973;56:150-161.

[50] Almquist KJ, Banks HT. A theoretical and computational method for determining optimal treatment schedules in fractionated radiation therapy. *Math Biosc* 1976;29:159-179.

[51] Norton L, Simon R. Tumor size, sensitivity to therapy, and design of treatment schedules. *Cancer Treat Rep* 1977;61:1307-1317.

[52] Norton L, Simon R. The Norton-Simon hypothesis revisited. *Cancer Treat Rep* 1986;70:163-169.

[53] Skipper HE, Schabel Jr FM, Wilcox WS. Experimental evaluation of potential anticancer agents. XIII. On the criteria and kinetics associated with "curability" of experimental leukemia. *Cancer Chemother Rep* 1964;35:1-111.

[54] Laird AK. Dynamics of tumor growth. *Br J Cancer* 1964;18:490-502.

[55] Burton AC. Rate of growth of solid tumors as a problem of diffusion. *Growth* 1966;30:157-176.

[56] Ang KK, Peters LJ, Weber RS, *et al.* Concomitant boost radiotherapy schedules in the treatment of carcinoma of the oropharynx andnasopharynx. *Int J Radiat Oncol Biol Phys* 1990;19:1339-1345.

[57] Peters LJ, Withers HR, Thames HD. Radiobiological bases for multiple daily fractionation. In: Karcher KH, Kogelnik HD, Reinartz G, editors. Progress in radio-oncology II. New York: Raven Press; 1982. p. 317-323.

[58] Knee R, Fields RS, Peters LJ. Concomitant boost radiotherapy for advanced squamous cell carcinoma of the head and neck. *Radioth Oncol* 1985;4:1-7.

[59] Peters LJ. Accelerated fractionation using concomitant boost: a contribution of radiobiology to radiotherapy. *Br J. Radiat* 1992;24 (Suppl.):200-203.

[60] Schwade J, Markoe A, Abitbol A, *et al.* Accelerating hyperfractionation for carcinoma of the head and neck. *Semin Radiat Oncol* 1992;2:51-53.

[61] Maciejewski B, Zajusz A, Pilecki B, *et al.* Escalated hyperfractionation and stimulation of acute mucosal reaction in radiotherapy for cancer of the oral cavity an orophyarnx. *Semin Radiat Oncol* 1992;2:54-57.

[62] Harari PM. Adding dose escalation to accelerated hyperfractionation for head and neck cancer. *Semin Radiat Oncol* 1992;2:58-61.

[63] Brown JM, Giaccia AJ. The unique physiology of solid tumors: Opportunities (and problems) for cancer therapy. *Cancer Res* 1998;58:1408-1416.

[64] Langer R, Conn H, Vacanti J, *et al.* Control of tumour growth in animals by infusion of an angiogenesis inhibitor. *Proc Natl Acad Sci USA* 1980;77:4331.

[65] Thompson WD, Shiach KJ, Fraser RA, *et al.* Tumors acquire their vaculature by vessel incorporation, not vessel ingrowth. *J Pathol* 1987;151:323-332.

[66] Khalil AA, Horsman MR, Overgaard J. The importance of determining necrotic fraction when studying the effect of tumor volume on tissue oxygenation. *Acta Oncol* 1995;34:297-300.

[67] Stadler P, Feldmann HJ, Creighton C, *et al.* Changes in tumor oxygenation during combined treatment with split-course radiotherapy and chemotherapy in patients with head and neck cancer. *Radiother Oncol* 1998;48:157-164.

Figure 1. The optimal design of a static fractionation scheme (for 10 fractions per week) can be viewed as a constrained optimization problem of maximizing the TCP subject to two BED constraints. The shaded region corresponds to the space of feasible regimens. The curves outside the feasible regions are TCP iso-curves. The parameter values are set so that HF is the optimal static policy, has both constraints binding, and achieves a TCP of 0.7.

Figure 2. The fractionation scheme that optimizes problem (14)-(16) over the class of policies that administers 10 fractions per week with eight-hour intervals each weekday. The policy applies a total of 66.81 Gy over six weeks. Distinctive characteristics of the optimal scheme are that Friday afternoon doses are very large, afternoon doses are larger than morning doses, and the Friday afternoon doses are intensified throughout the course of treatment.

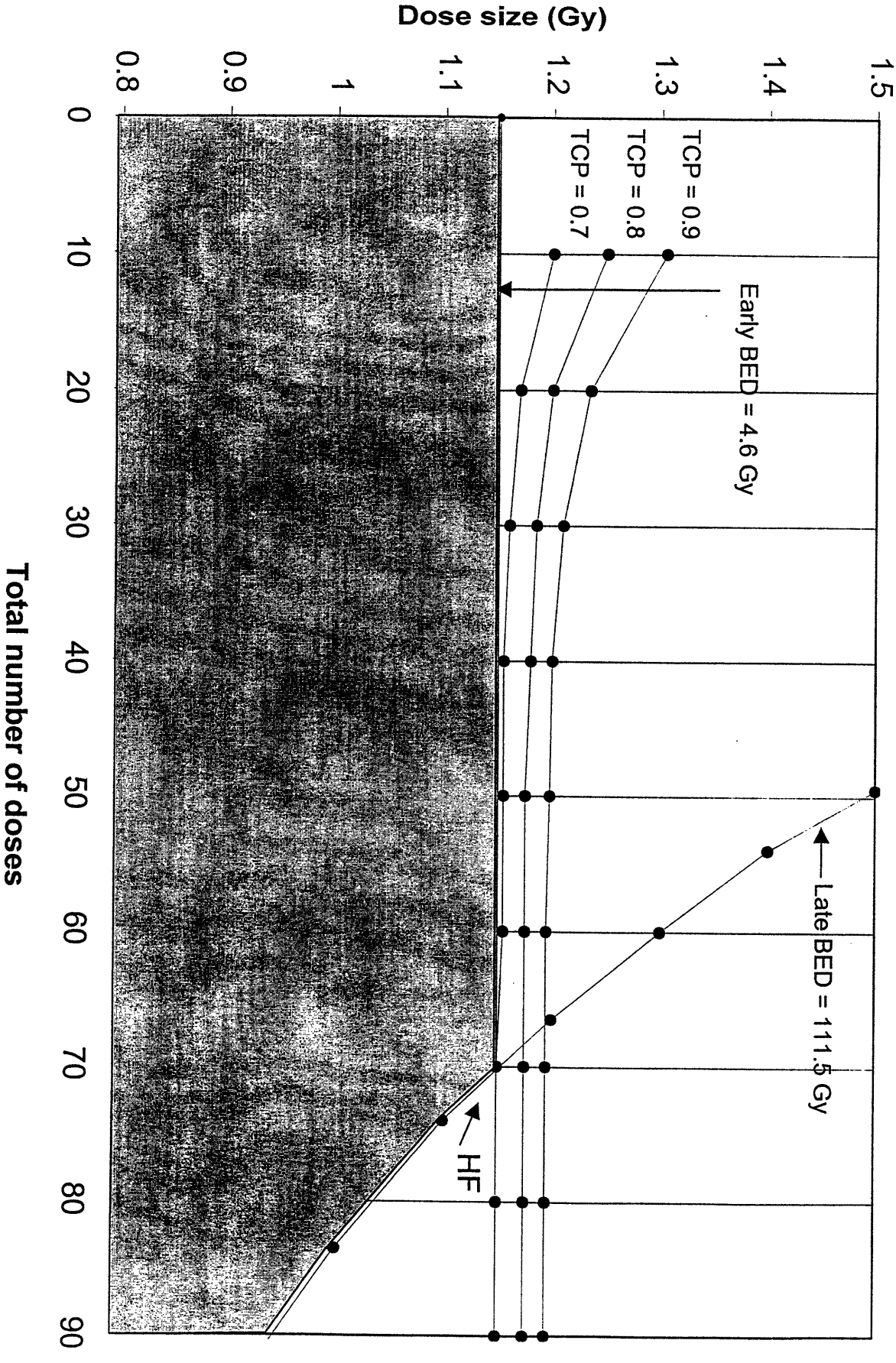
Dose size (Gy)
1.5
1.4
1.3
1.2
1.1
1
0.9
0.8
TCP = 0.9
TCP = 0.8
TCP = 0.7
Early BED = 4.6 Gy
Late BED = 111.5 Gy
HF
0
10
20
30
40
50
60
70
80
90
Total number of doses

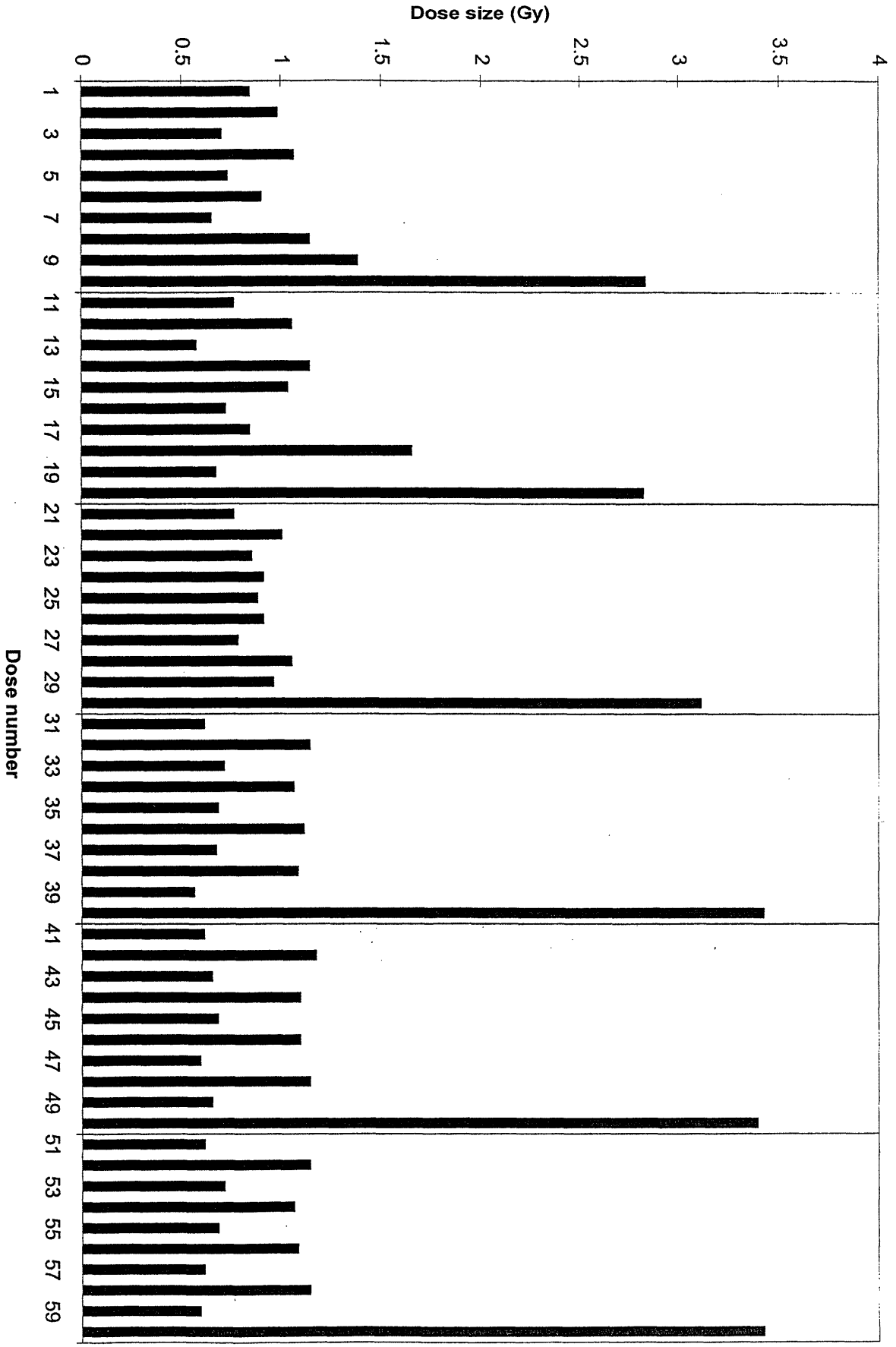
Dose size (Gy)
0
0.5
1
1.5
2
2.5
3
3.5
4
Dose number
1 3 5 7 9 11 13 15 17 19 21 23 25 27 29 31 33 35 37 39 41 43 45 47 49 51 53 55 57 59